Electronic Supplementary Material (ESI) for Journal of Materials Chemistry A.

Supporting Information

Low ion-transfer resistance and high volumetric supercapacitor using hydrophilically surface modified carbon electrodes

*Heejoun Yoo,Misook Min,Sora Bak,Yeoheung Yoon and Hyoyoung Lee**

Table S1. Comparison of capacitance of the rGO/CNTs electrode in literature data.

Ref.	Charateristics	Electrolyte, system	Gravitic Capacitance	Volumetric Capacitance
1	rGO/SWCNT	BMIM BF_4, 2 electrode	222 F g^{-1} at 1 A g^{-1}	-
2	rGO/MWCNT, self-assembled	1M H_2SO_4, 3 electrode	279 F g^{-1} at 1 A g^{-1}	-
3	GO/MWCNT	1M H_2SO_4, 3 electrode	180 F g^{-1} at 0.4 A g^{-1}	-
4	rGO/MWCNT, amin functionalized	0.5M H_2SO_4, 3 electrode	175 F g^{-1}	-
5	rGO/MWCNT film	6M KOH, 3 electrode	265 F g^{-1} at 0,1 A g^{-1}	-
6	rGO/MWCNT, Poly(ethylenimine) assited	1M H_2SO_4, 3 electrode	120 F g^{-1} at 1 V s^{-1}	-
7	rGO/SWCNT	1M KCl, 2 electrode	201 F g^{-1} at 0.5 A g^{-1}	-
8	rGO/MWCNT	3M KCl, 2 electrode		6.1 mF cm^{-2}

Table S2. Comparison of capacitance of solid-state supercapacitors demonstrated in this study with literature data.

Ref	Characteristics	Electrolyte, System	Capacitance / F g^{-1}	Volumetric Capacitance	Mass loading	Electrode thickness
9	SWCNT, printable film	PVA-H_3PO_4	110 F g^{-1}	3.62 cm^{-2}	33.3 μg cm^{-2}	~ 0.6 μm
10	rGO, Laser scribing	PVA-H_3PO_4	203.8 F g^{-1}	7.34 cm^{-2}	36.3 μg cm^{-2}	~ 7.6 μm
11	rGO, cellulose composite paper	PVA-H_3PO_4	68.1 F g^{-1}	46 cm^{-2}	680 μg cm^{-2}	-
12	rGO, Hydrogel solide-state	PVA-H_2SO_4	93 F g^{-1}	372 F cm^{-2}, 6.25 F cm^{-3}	2000 μg cm^{-2}	~ 185 μm
13	rGO pattern	PVA-H_3PO_4	285 F g^{-1}	0.462 F cm^{-2}, 359 F cm^{-3}	0.315 μg cm^{-2}	0.025 μm
This work	RGO-SCNT25	PVA-H_3PO_4	53.2 F g^{-1}	85 F cm^{-2}, 50 F cm^{-3}	1600 μg cm^{-2}	17 μm
	RGO-SCNT50	PVA-H_3PO_4	45.2 F g^{-1}	81 F cm^{-2}, 40 F cm^{-3}	1800 μg cm^{-2}	20 μm

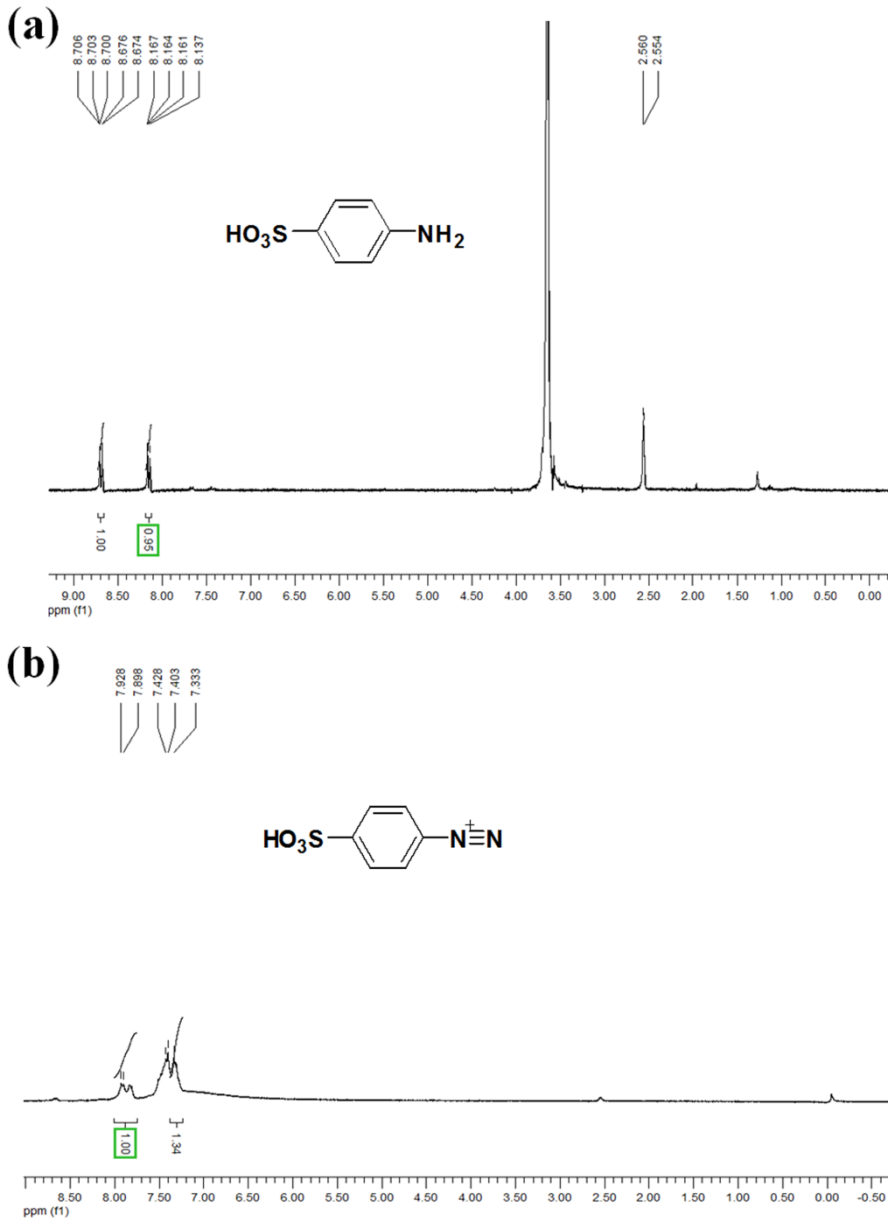

Fig. S1. The 1H spectra of (a) *p*-sulfonic acid and (b) 4-Benzenediazoniumsulfonate.

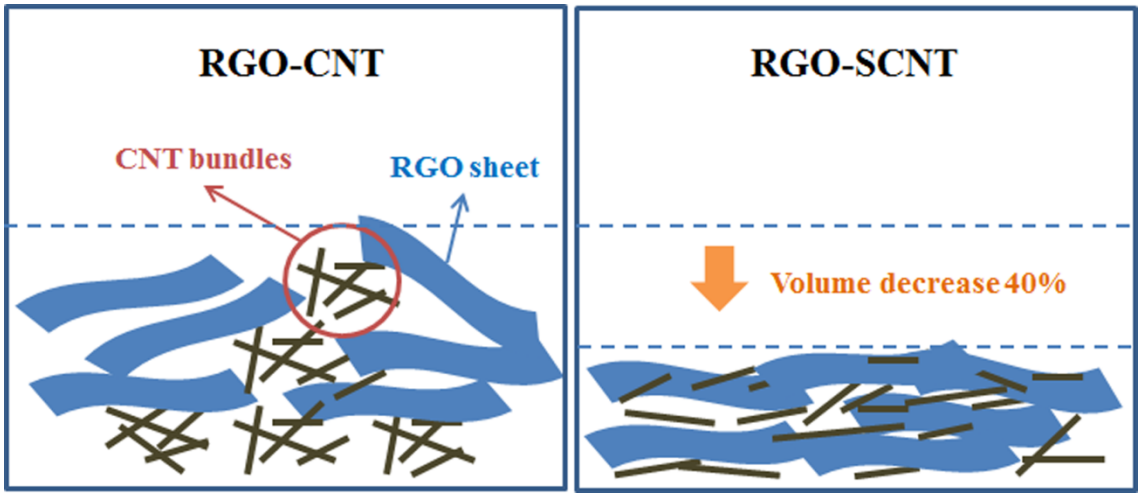

Fig. S2. The schematic images of RGO-CNT and RGO-SCNT electrodes.

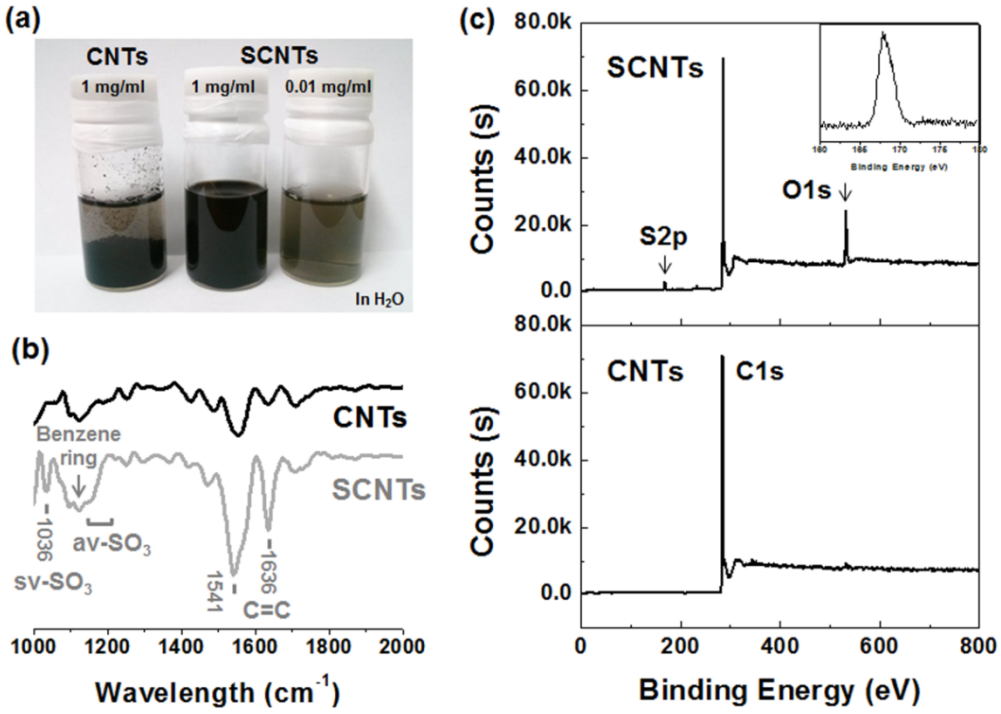

Fig. S3. (a) Optical image of CNTs and SCNTs dispersion solution in H_2O. (b) FT-IR spectra of CNTs and SCNTs. (c) XPS spectra of CNTs and SCNTs.

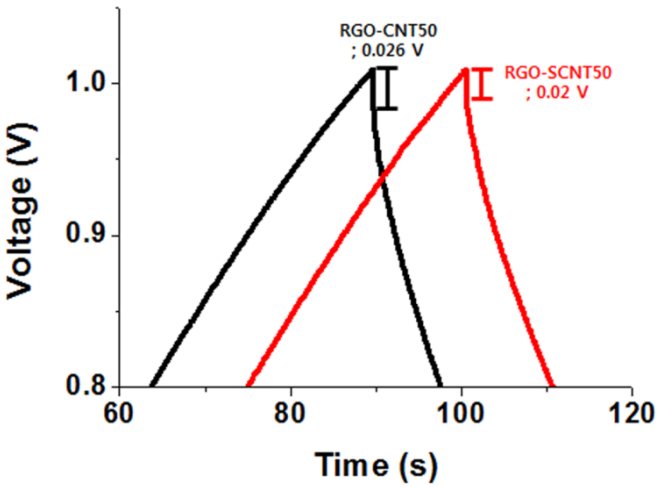

Fig. S4. Voltage drops of galvanostatic charge-discharge for RGO-CNT50 and RGO-SCNT50.

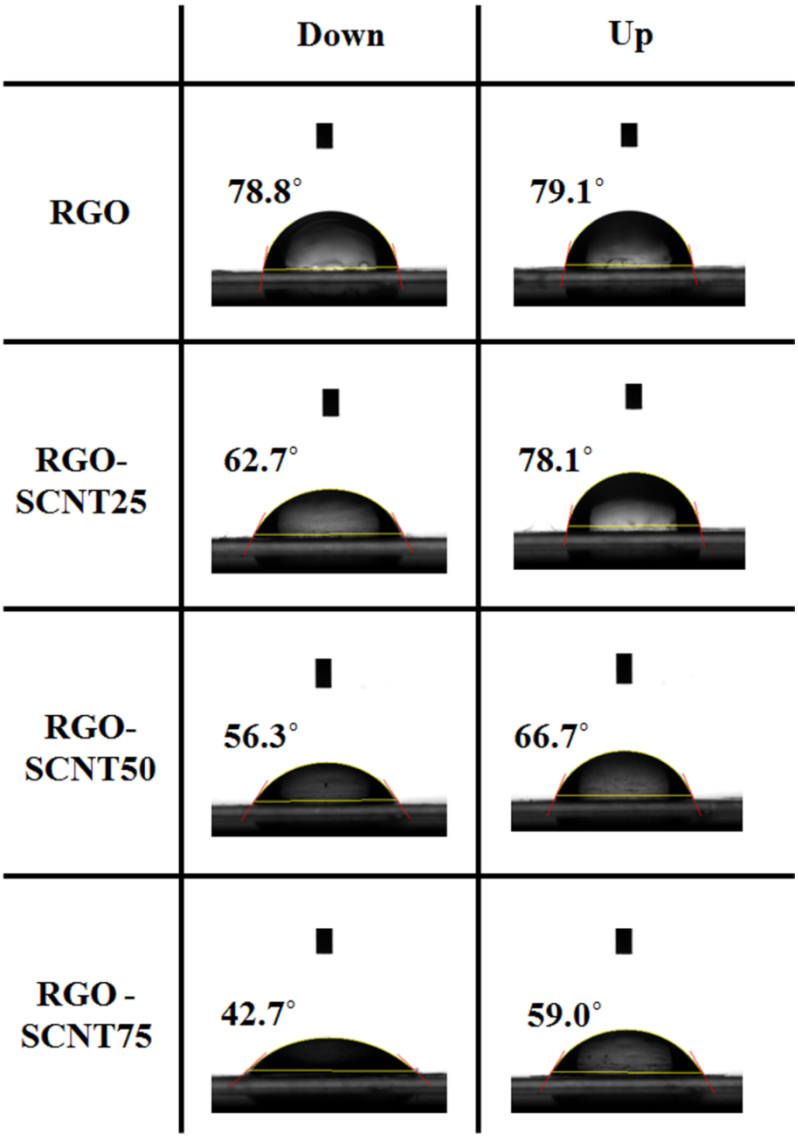

Figure S5. The comparison water contact images (down and upside) of RGO, RGO-SCNT25, RGO-SCNT50, and RGO-SCNT75.

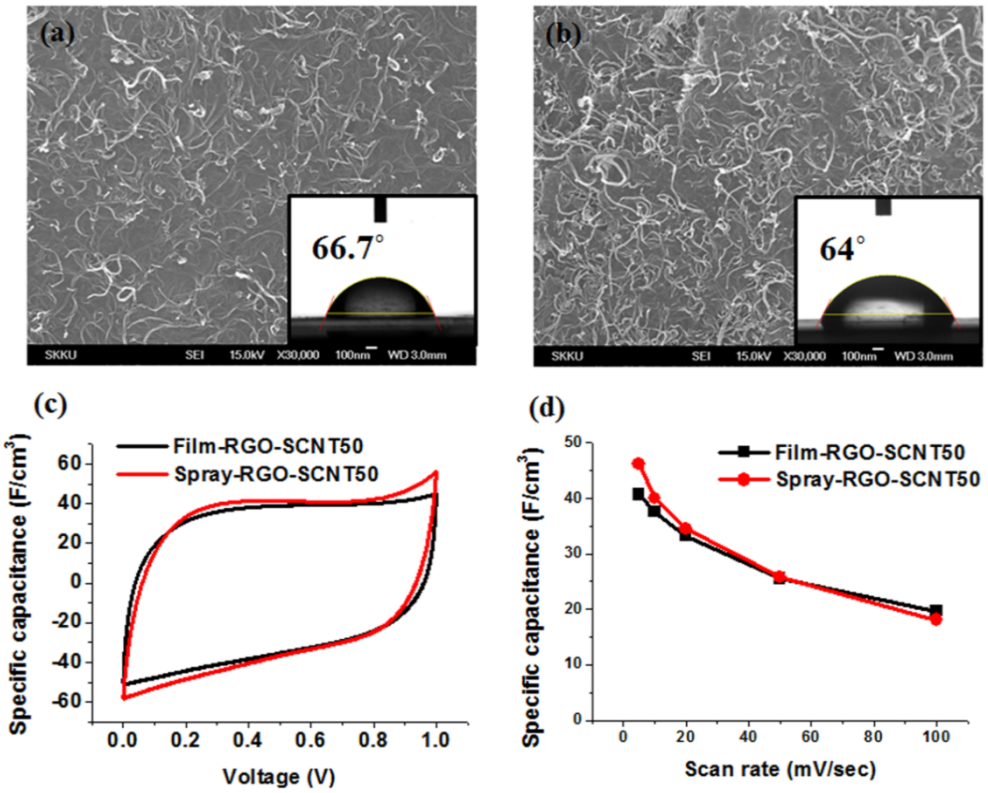

Fig. S6 The SEM images and water contact angle (inset) of (a) film-RGO-SCNT50, (b) spray-RGO-SCNT50, (c) CV curves at scan rate of 20 mV sec^{-1}, (d) Volumetric capacitance with different scan rate from 2 to 100 mV sec^{-1}.

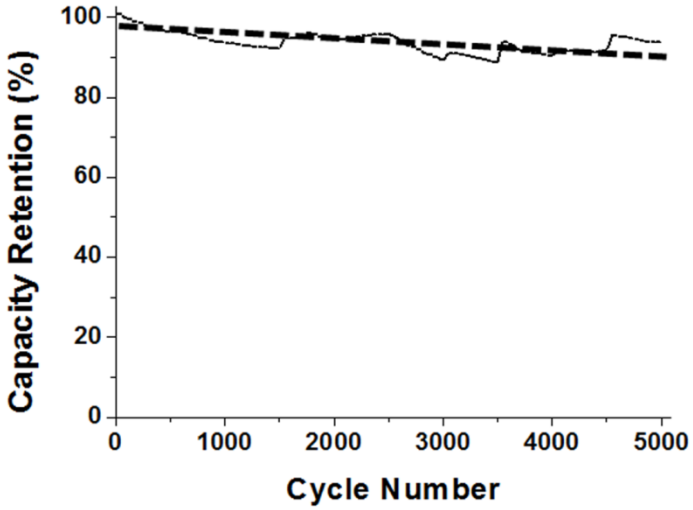

Fig. S7 Cycling stability of the RGO-SCNT50 at 100mV sec^{-1}

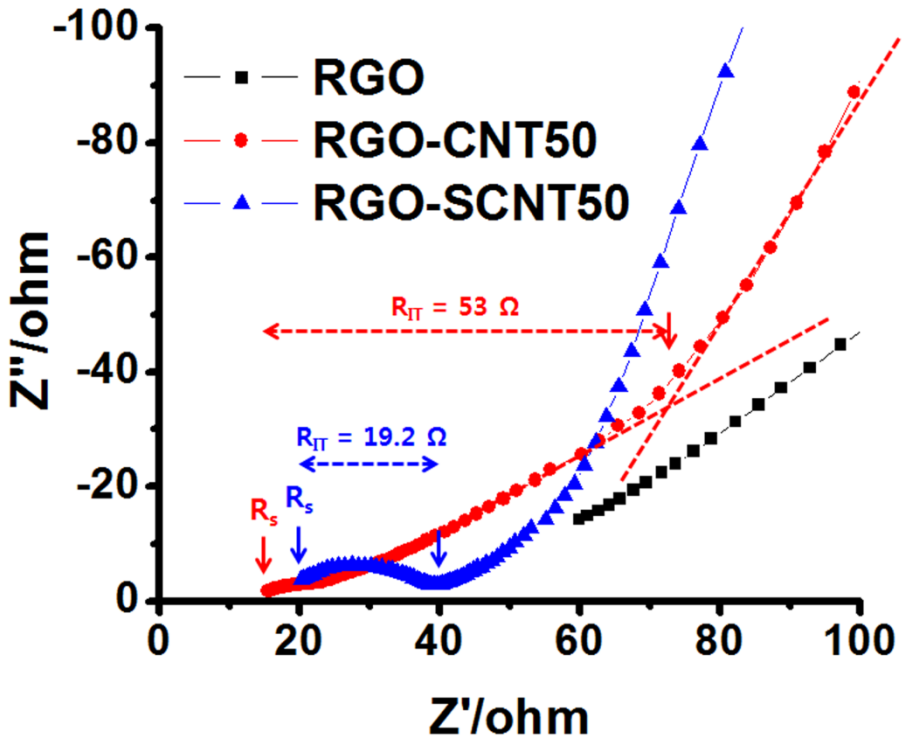

Fig. S8 Nyquist impedance plots and fitting data for R_s and R_{IT}.

Table S3. The specification and capacitance data of solid-state supercapacitors demonstrated in this study.

	Electrode specification				Specific capacitance [a]			Water contact angles		Resistance (Ω) [b]	
	CNT ratio (wt%)	Weight (mg)	Thickness (μm)	Bulk density (g cm^{-3})	Volumetric (F cm^{-3})	Areal (mF cm^{-2})	Gravimetric (F g^{-1})	Down side	Top side	R_S	R_{IT}
RGO	-	2	18	1.11	6.3	10.6	5.3	78.8	79.1	60	~380
RGO-CNT50	50	2.1	40	0.53	18.5	74	35.2	82.4	89.8	15.5	53
RGO-SCNT25	25	1.6	17	0.94	50.1	85.2	53.2	62.7	78.1	20.8	~ 60
RGO-SCNT50	50	1.8	20	0.9	40.7	81.4	45.2	56.3	66.7	20.2	19.2
RGO-SCNT75	75	1.8	28	0.64	16.8	47.1	26.2	42.7	59	24.6	12.3
Spray-RGO-SCNT50	50	0.7	10	0.7	46.2	46.2	66.1	-	-	-	-

a) Calculated from the CV curves at 5 mV sec^{-1}; b) Obtained from the Nyquist impedance plots

Reference

1 N. Jha, P. Ramesh, E. Bekyarova, M. E. Itkis, R. C. Haddon, Adv. Energy Mater., 2012, 2, 438.

2 Z-D. Huang, B. Zhang, S-W. Oh, Q-B. Zheng, X-Y. Lin, N. Yousefi, J-K. Kim, J. Mater. Chem., 2012, **22**, 3591.

3 S. H. Aboutalebi, A. T. Chidembo, M. Salari, K. Konstantinov, D. Wexler, H. K. Liu, S. X. Dou, Energy Environ. Sci., 2011, **4**, 1855.

4 H. R. Byon, S. W. Lee, S. Chen, P. T. Hammond, Y. Shao-Horn, Carbon, 2011, **49**, 457.

5 X. Lu, H. Dou, B. Gao, C. Yuan, S. Yang, L. Hao, L. Shen, X. Zhang, Electrochimica Acta, 2011, **56**, 5115.

6 D. Yu, L. Dai, J. Phys. Chem. Lett., 2010, **1**, 467.

7 Q. Cheng, J. Tang, J. Ma, H. Zhang, N. Shinya, L-C. Qin, Phys. Chem. Chem. Phys., 2011, **13**, 17615.

8 M. Beidaghi, C. Wang, Adv. Funct. Mater., 2012, **22**, 4501.

9 M. Kaempgen, C. K. Chan, J. Ma, Y. Cui, G. Gruner, Nano Letters, 2009, **9**, 1872.

10 M. F. El-Kady, V. Strong, S. Dubin, R. B. Kaner, Science, 2012, **335**, 1326.

11 Z. Weng, Y. Su, D-W. Wang, F. Li, J. Du, H-M. Cheng, Adv. Energy Mater., 2011, **1**, 917.

12 Y. Xu, Z. Lin, X. Huang, Y. Liu, Y. Huang, X. Duan, ACS Nano, 2013, **7**, 4021.

13 Z. Niu, L. Zhang, L, Liu, B. Zhu, H. Dong, X. Chen, Adv. Mater. 2013, **25**, 4035.